Ecological Engineering 60 (2013) 276–288

Contents lists available at ScienceDirect

Ecological Engineering

journal homepage: www.elsevier.com/locate/ecoleng

Deciphering and modeling the physicochemical drivers of denitrification rates in bioreactors

Casey A. Schmidt[a,*], Mark W. Clark[b]

[a] Desert Research Institute, 2215 Raggio Parkway, Reno, NV, USA
[b] Soil and Water Science Department, University of Florida, 2181 McCarty Hall, PO Box 110290, Gainesville, FL, USA

ARTICLE INFO

Article history:
Received 1 March 2013
Received in revised form 20 June 2013
Accepted 6 July 2013
Available online 17 August 2013

Keywords:
Denitrification wall
Bioreactor
Groundwater
Denitrification rate
Multivariate analysis
Temperature
Surface area
Carbon quality

ABSTRACT

Denitrification bioreactors have served as effective artificial N sinks by stimulating denitrification and remediating excessive nitrate. Predictions on bioreactor performance will be improved by quantifying the relationship between denitrification rates and causal factors which vary by geography (temperature), land-use intensity (NO_3 concentration) and media type (carbon quality, quantity, and surface area). Experimental mesocosms filled with different wood media types (oak, pine), particle sizes and wood–sand volume ratios were exposed to flowing high-nitrate groundwater across a range of seasonal groundwater temperatures (8–24 °C) to determine the influence of these coarse but utilitarian parameters on bioreactor performance. To increase the transferability and specificity of findings, a multivariate analysis was used to quantify relationships between denitrification rates, microbial biomass, temperature, media surface area to volume ratio and metrics of C quality to guide de novo media selection and performance predictions. There were no strong differences in hydraulic conductivity, media consumption rates, and TKN flux between different treatments although increasing the wood–sand volume ratio alone produced significant increases in denitrification rates and undesirable DOC leaching. Fluxes of DOC and TKN also increased with higher hydraulic loading rates. Denitrification rates were unresponsive to nitrate concentration and most strongly influenced by groundwater temperature (Q_{10} = 4.7), although carbon bioavailability and media surface area were uniquely predictive of denitrification rates. Bioreactor performance will therefore be most strongly influenced by geographical variations in temperature, although within a specific location, bioreactor media selection will influence denitrification rates.

© 2013 The Authors. Published by Elsevier B.V. Open access under CC BY-NC-ND license.

1. Introduction

The use of N-based fertilizer will need to increase to meet future demands for agricultural crops (Tenkorang and Lowenberg-DeBoer, 2009), yet existing N application rates have been implicated as the main source of coastal eutrophication (Howarth and Marino, 2006) and a significant contributor to the growth of large hypoxic dead zones in regions such as the Gulf of Mexico (Goolsby and Battaglin, 2000) and Chesapeake Bay (Hagy et al., 2004). Producing sufficient crops to feed a growing planet will require efficient food production in combination with innovative and sustainable practices to protect aquatic ecosystems. The long-term success of carbon-based denitrification bioreactors (Long et al., 2010; Moorman et al., 2010; Robertson et al., 2008) to create hotspots of biological denitrification (Warneke et al., 2011a), and cost-effectively and efficiently remove nitrate (NO_3) from groundwater with limited maintenance, indicates this technology is a feasible treatment option. Denitrification bioreactors have generally taken the form of; lined beds filled with woodchips used to treat point sources of agricultural effluent, and denitrification walls where wood chips or sawdust were mixed with the soil in a permeable reactive barrier (PRB) to treat non-point sources (Schipper et al., 2010). To supplement the application of denitrification walls where non-point N is the concern (Schmidt and Clark, 2012a,b), factors affecting denitrification wall performance were examined.

Bioreactor denitrification rates are influenced by a variety of factors including the relatively immutable site specific factors

Abbreviations: CPS, coarse pine sawdust treatment; FPS, fine pine sawdust treatment; OS, oak sawdust treatment; LCI, lignocellulose index; LOI, loss on ignition; MBC, microbial biomass carbon; NDF, neutral detergent fiber; PRB, permeable reactive barrier; ShrP, shredded pine treatment; TKN, total Kjeldahl nitrogen; DOC, dissolved organic carbon.

* Corresponding author. Tel.: +1 775 673 7464; fax: +1 775 673 7363.
E-mail addresses: casey.schmidt@dri.edu (C.A. Schmidt), clarkmw@ifas.ufl.edu (M.W. Clark).

0925-8574 © 2013 The Authors. Published by Elsevier B.V. Open access under CC BY-NC-ND license.
http://dx.doi.org/10.1016/j.ecoleng.2013.07.041

such as the groundwater temperature and influent nitrate concentration and the type and properties of media. Previous research has indicated that wood media sustains adequate denitrification rates over longer time spans and has fewer adverse effects (N_2O emissions, TKN, DOC export) as compared to more labile media (maize cobs, wheat straw, green waste) (Cameron and Schipper, 2010; Long et al., 2010; Schipper and Vojvodic-Vukovic, 2001; Warneke et al., 2011c). As a result, wood has been the most common media used. Denitrification wall media has included; hardwood (Robertson et al., 2000) and softwood sawdust (Schipper and Vojvodic-Vukovic, 1998; Schmidt and Clark, 2012a,b) wood chips (Jaynes et al., 2008) and with volume mix ratios of wood to sand ($v_{wood}/v_{total\ media}$; wood volume ratio) of 0.20 (Robertson and Cherry, 1995; Schipper et al., 2004), 0.50 (Schipper and Vojvodic-Vukovic, 1998) and 1.0 (Fahrner, 2002). Predictions on bioreactor performance and denitrification rates within a specific site can be improved by assessing and quantifying influential media properties which affect nitrate removal rate, microbial biomass and denitrification enzyme activity. Additionally, some bioreactors have been hampered by the occurrence of unintended negative consequences that may be correlated to media properties such as undesirable variations in hydraulic conductivity (Schipper et al., 2004), as well as excess dissolved organic C (DOC) and total Kjeldahl N (TKN) export (Cameron and Schipper, 2010; Schmidt and Clark, 2012a,b). Determining the impacts resulting from variations in commonly available wood types (oak, pine), sizes (sawdust, chips, etc.) and wood volume ratio will improve predictions on groundwater denitrification rates and the potential occurrence of adverse effects in denitrification walls.

Bioreactor guidelines based on wood type, particle size and wood volume ratios may have a pragmatic, albeit limited utility because general wood properties which could affect denitrification rate and microbial populations (C availability, surface area/porosity) can vary due to differences in species, age (Robertson, 2010), plant components, preparation methods, and climate of the growing region (Kilpelainen et al., 2003). The profuse application of bioreactors can be facilitated by predictions based solely on measurable physicochemical drivers of microbial properties and nitrate reduction rates. Previous researchers have made inferences on the influence of wood surface area and C bioavailability on denitrification rates in bioreactors utilizing metrics of wood grain size (Cameron and Schipper, 2010), respirable C (Schipper and Vojvodic-Vukovic, 2001; Warneke et al., 2011b,c) and C:N ratio (Greenan et al., 2006). Warneke et al. (2011c) showed that respirable C was positively correlated with denitrification rate, although the specific properties of the media that influence C respiration weren't determined. Guiding de novo media selection requires determining the proximate causal wood media properties which influence denitrification rate and microbial activity. Greenan et al. (2006) observed that media which had a lower C:N ratio and presumably lower lignin content tended to have higher denitrification rates, although this relationship wasn't quantified. Quantifying and interpreting foundational C bioavailability metrics which are uniquely correlated with denitrification rate will improve our understanding of microbial processes and facilitate predictions of bioreactor performance.

The influence of media surface area on denitrification rates has also been examined. The surface area in a given volume (surface area to volume ratio) of wood media could plausibly influence denitrification rates due to an increased area for extracellular enzyme exposure and bacterial colonization. Because the surface area to volume ratio is inherently related to grain size, researchers have compared media of differing grain sizes and they have found a weak to non-detectable influence on denitrification rates (Cameron and Schipper, 2010; Robertson et al., 2000). Grain size is not always a strong determinant of the surface area due to variations in the effective porosity of the wood, therefore surface area alone needs to be quantified to accurately decipher this relationship.

Predictions on bioreactor performance based on wood media properties alone will need to incorporate the variability in groundwater temperature and influent nitrate concentrations at installation sites, which both affect denitrification reaction kinetics (Cameron and Schipper, 2010; Elgood et al., 2010; Robertson et al., 2008; Robertson, 2010; van Driel et al., 2006a,b; Warneke et al., 2011b,c). The correlation between temperature and denitrification rates has been hypothesized as an exponential relationship with a doubling of denitrification rates every 10 °C ($Q_{10} = 2.0$), although Q_{10} values for denitrification rates have varied by an order of magnitude (0.16–4.95) (Cameron and Schipper, 2010; Elgood et al., 2010; Robertson et al., 2008; Warneke et al., 2011c). Similarly, the relationship between nitrate concentration and denitrification rate has been hypothesized to be non-linear following Michaelis–Mentin kinetics. Some studies have failed to confirm this (Robertson, 2010; Warneke et al., 2011b), while another study found a strong influence of nitrate concentration on denitrification rates (Christianson et al., 2012). Further controlled studies will be required to quantify these relationships.

In the following study, nitrate-N removal rates were evaluated in experimental mesocosms filled with different wood media types, sizes and wood volume ratios for 246 days. Water samples were collected at several locations within the mesocosm to assess the influence of declining nitrate-N concentrations on the kinetics of the denitrification reaction. Groundwater temperature was measured during each sampling event to determine the covariance of temperature and each treatment. The differences in nitrate-N removal rates and the occurrence of adverse effects (low hydraulic conductivity, DOC and TKN export) were evaluated between treatments (type, size, and volume ratio) to provide pragmatic guidelines on bioreactor implementation utilizing commonly available wood media. Empirical relationships between predictive metrics of bioreactor media (total C, C:N ratio, surface area and fiber quality) were quantified to determine whether C quality and/or quantity significantly increases TKN and DOC production, microbial biomass and experimental and laboratory measures of denitrification rates. Because metrics of surface area, C quality and quantity may be cross-correlated, a step-wise multivariate analysis was utilized to filter cross-correlated variables and construe the parameters which had discrete and strong contributions to measured nitrate-N removal rates and estimates of microbial biomass. From these results a statistical model was developed to provide transferable predictions on bioreactor performance from measurable predictor variables.

2. Materials and methods

2.1. Experimental design

Groundwater from underneath an agricultural property described in Schmidt and Clark (2012a,b), with an average nitrate-N concentration of 7.5 ± 0.73 mg L^{-1} continuously flowed vertically through PVC mesocosms (diameter 15.2 cm, length 152 cm) filled with different wood types, particle sizes and volume ratios ($v_{wood}/v_{total\ media}$) for 246 days (Fig. 1). The groundwater was pumped from a well to a sealed bladder contained within a water bath, protected from atmospheric exposure, and discharged through the treatments via precisely controlled head gradients (Fig. 1). The experimental unit was covered with a tent and each individual external component was wrapped with reflective and

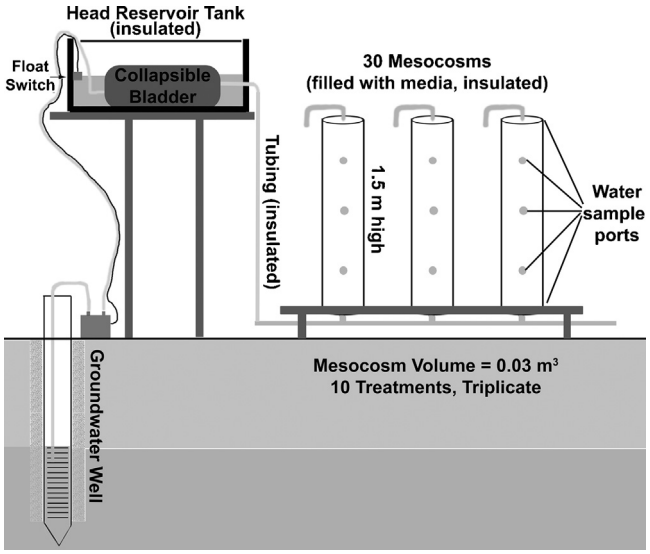

Fig. 1. A diagram of the experimental design. Groundwater from underneath an agricultural property continuously flowed through 30 mesocosms filled with different wood types, sizes and volume ratios for 246 days. Groundwater was protected from exposure to oxygen and temperature fluctuations.

insulated material to reduce temperature changes. Temperature of influent and effluent water was measured at each sampling event.

Treatments were prepared by thoroughly mixing the wood with a washed and sieved quartz sand (particle size = 0.106–0.15 mm), adding the media to the mesocosm and tamping down with a consistent pressure every 0.3 m. Subsamples of media were collected in duplicate at the beginning of the study for quality control and for comparison to media collected at the end of the study. Ten different treatments were analyzed in triplicate (Table 1) including four different sizes of commonly available wood media, two wood types (oak, pine) and four different wood volume ratios (0, 0.10, 0.25, and 0.50) (Table 1). Wood mass ratios averaged 4.3 ± 1.4, 11 ± 6.3, and 19 ± 4.2% for the 0.10, 0.25, and 0.50 treatments, respectively. Variations in wood amount, size and type allowed for qualitative comparisons of the treatments, while also producing quantitative variability in the physicochemical parameters (total C, C quality metrics and surface area) which were potentially correlated with denitrification rates and microbial biomass.

2.2. Bioreactor media hydraulic properties

The pore volume which transmits groundwater (effective porosity), was determined as the volume of water that drained due to gravity from previously saturated mesocosms (Ahuja et al., 1984; Barkle et al., 2007; Fetter, 2001; Timlin et al., 1999). Saturated hydraulic conductivity (K_{sat}) was measured over time ($n = 11$) using the constant head method (ASTM, 2006) and quantified with a modified form of Darcy's equation.

2.3. Water sampling and analysis

Fluxes of nitrate, TKN and DOC were evaluated by collecting water samples nine times (days 0, 9, 36, 59, 86, 141, 176, 183, and 246) every 38 cm within the mesocosm through water sampling ports that were covered with a 0.155 mm nylon fabric to prevent the fluidized reactor media from mobilizing. For quality assurance, six duplicate samples were collected at each sampling event and to determine if there was horizontal variability resulting from short-circuiting, nine randomly distributed sampling ports were duplicated. Each sample was collected as both an unfiltered, acidified sample and a sample that was passed through a 0.45 μm membrane filter (Pall Corporation, Port Washington, NY), then acidified. Samples were immediately stored on wet ice, transported to the laboratory and placed in a refrigerator at 4 °C until analysis within 28 days. Unfiltered samples were processed using a block digestion and analyzed colorimetrically for TKN (EPA Method 351.2) and filtered samples were analyzed colorimetrically (EPA Method 353.2) after cadmium reduction, both using an autoanalyzer (Seal Analytical, West Sussex, UK). Total organic C was quantified on filtered samples using EPA Method 415.1, after combustion as non-purgable organic C with an infrared gas analyzer (Shimadzu Corp, Kyoto, Japan).

Changes in nitrate-N, DOC and TKN within the treatments were determined as the difference in, mass flux rates between the sampling ports and normalized per volume of reactor media using Eq. (1):

$$N_r,\ DOC_e,\ TKN_e = \frac{Q\Delta[N],\ [DOC],\ [TKN]}{V_s} \quad (1)$$

In this equation, N_r, DOC_e, and TKN_e are the reduction in nitrate-N, and increase in DOC and TKN mass flux rates in effluent water per volume of reactor media [M-NO_3-N/DOC/TKN $L^{-3}\,T^{-1}$], Q is the mesocosm discharge [$L^3\,T^{-1}$], Δ[N], [DOC][TKN] are the change in analyte concentration between sampling ports [$M\,L^{-3}$] and V_s is the mesocosm volume the groundwater travels through [L^3].

DOC export rates had a declining trend over time. Therefore to estimate total DOC export, measured values were fit to an exponential decay model in JMP® 8.0 (SAS Institute Inc., Cary, NC) with Eq. (2):

$$C_t = C_o\, e^{-rt} + \theta \quad (2)$$

In this equation, C_t is the DOC export rate per volume of media at time t [$M\,L^{-3}\,T^{-1}$], C_o is the initial DOC export rate at $t = 0$, r is the

Table 1
A summary of the bioreactor media treatments. The particle diameter range is described as the D_{25}, D_{50} and D_{75}, which is the particle diameter below which 25, 50 (mean) and 75% of the media was finer by mass.

Wood type	Wood vol. ratio (v_{wood}/v_{total})	Diameter (D_{25}, D_{50}, D_{75}) (mm)	Species	Porosity (%)	Bulk dens. (g cm^{-3})	%C	%N	C:N
Fine pine sawdust	0.10			52	1.6	1.63	0.011	148
Fine pine sawdust	0.25	(0.35, 0.53, 0.55)		60	1.1	3.37	0.013	259
Fine pine sawdust	0.50		*Pinustaeda, elliottii*	52	0.8	7.42	0.032	232
Coarse pine sawdust	0.10			47	1.6	2.38	0.011	216
Coarse pine sawdust	0.25	(1.4, 2.5, 4)		50	1.6	3.96	0.021	189
Coarse pine sawdust	0.50			61	1.3	10.4	0.054	193
Shredded pine	0.25	(3.5, 6.3, 7.8)		71	1.3	9.41	0.018	523
Oak sawdust	0.25	(0.17, 0.41, 0.79)	*Quercusnigra, virginiana*	66	1.2	3.55	0.022	161
Oak sawdust	0.50			77	0.9	8.59	0.057	151
Control sand	0.00	(0.11–0.22)		38	1.8	0.247	0.000	

exponential rate constant and θ is the asymptote rate. The variable θ was manually fit as the average DOC export rate in the final two sampling events.

2.4. Bioreactor media sampling

Bulk density was quantified as the dry weight divided by the mesocosm volume. Subsamples of the reactor media were collected from each treatment in duplicate at day 0 before groundwater exposure and at day 246 at five locations (0, 10, 38, 76 and 114 cm) in each mesocosm. Media samples were collected in bags, immediately placed in wet ice and brought back to the laboratory to be stored at 4 °C until analysis. Samples collected at the beginning of the study were evaluated for total C, N, fiber components and micropore and macropore surface area and their predictive capacity on bioreactor performance was evaluated. Samples collected at the end of the study were analyzed for microbial biomass C, and potential denitrification rate to infer biological activity; and total C, N and fiber components were quantified to assess temporal changes to the media. The matrix of sand and shredded pine was too heterogeneous to collect a representative sample at the end of the study with a coring device, therefore this treatment was excluded from the temporal media change analysis.

2.5. Carbon quality analysis

The gravimetric moisture content was quantified by weighing a fresh subsample in a forced air drying oven at 105 °C for 48 h. Oven-dried samples were homogenized and processed with a plant grinder for fiber analysis (Thomas Scientific, Swedesboro, NJ) and subsamples of dried and ground media were further grinded with a ball-mill. Neutral detergent fiber (NDF), hemicellulose, cellulose and lignin were quantified as mass loss after a sequential neutral detergent-acid digestion (Van Soest et al., 1991) in a fiber analyzer (ANKOM, Fairport, NY). Mineral content was calculated after 4 h in a 550 °C muffle furnace as the mass remaining after ignition. Total C and total N were quantified using a thermal conductivity detector after dynamic flash combustion (Flash EA® 1112, Thermo Fisher Scientific, Miami, OK).

2.6. Microbial biomass carbon

Moist media samples were analyzed for microbial biomass C (MBC) by the 24 h chloroform fumigation-extraction method within 4 days (Vance et al., 1987). Samples were extracted with 25 mL of 0.5 M K_2SO_4, filtered through 2.5 μm filter paper (Whatman, Maidstone, UK), measured for total organic C (TOC), and calculated as the difference between untreated and chloroform-fumigated media with an extraction efficiency (k_{EC}) factor of 0.37 applied based on previous determinations (Sparling et al., 1990).

2.7. Media potential denitrification rate

Potential denitrification rate was quantified in triplicate within each mesocosm using methods described previously (Schmidt and Clark, 2012a). Homogenized soil slurries were inundated with influent groundwater only (NO_3 = 7.9, TKN = 0.35, DOC = 0.83 mg L^{-1}) that was purged with 99.99% O_2-free N_2 gas, approximately 15% of the headspace was replaced with acetylene gas (C_2H_2) and samples were shaken on a longitudinal shaker and kept consistently at 22 °C. Headspace gas was sampled after 4 h, then hourly for 5 h and rates were quantified by fitting a regression line to cumulative N_2O production and normalized as a rate per media volume.

N_2O production in headspace gas was quantified with a gas chromatograph, equipped with a 3.7 × 108 (10 mCi) 63NI electron capture detector (300C) (Shimadzu GC-14A, Kyoto, Japan), a stainless steel column (1.8 m long by 2 mm i.d.) packed with Poropak™ Q (0.177–0.149 mm; 80–100 mesh) (Supelco, Bellefonte, PA) with operating temperatures of 120, 30 and 230 °C for the injector, column and detector, respectively. All values were modified to account for N_2O dissolution into the aqueous phase employing Bunsen absorption coefficients (Tiedje, 1982).

2.8. Media surface area

Media surface area was quantified on an autosorb® (Quantachrome, Boynton Beach, Florida) with N_2 and CO_2 sorptometry using methodology described extensively in Mukherjee et al. (2011). A surface area including only nanopores (>2 nm diameter) was quantified with the probe gas N_2 at 77 K and the surface area including nanopores and micropores (<2 nm diameter) was measured at 273 K with CO_2 as the probe gas.

2.9. Statistical and data analysis

Media C and fiber consumption rates between day 0 and day 246 were discerned between treatments on a pool of differences within individual mesocosms (matched pair analysis). Nitrate-N reduction rates between treatments (wood size, type, and volume ratio) were modeled as an analysis of covariance (ANCOVA), controlling for a covarying temperature interaction using the PROC GLM procedure (SAS® 9.2, SAS Institute Inc., Cary, NC). Relationships between numeric continuous predictor variables (e.g. fiber composition, total C, C:N ratio, and surface area) and response variables (nitrate-N reduction rates and microbial biomass C) were analyzed using bivariate correlations and multiple regression. Because many predictor variables were inherently cross-correlated, a bidirectional stepwise regression was used to screen and select strong and uniquely predictive variables. Using multiple regression, results were analyzed as a linear combination of screened predictor variables to create a model of nitrate-N removal rates based on a minimal number of discrete predictors. Predictor variables which had non-linear relationships (e.g. temperature, surface area) were modeled using the fit model platform. Prior to model construction, two mesocosm treatments were randomly chosen from each sampling day (n = 12), removed from model construction and used as a verification dataset by analyzing as a linear regression between measured and predicted responses. All analyses were done at an alpha level of 0.05 and pairwise t-tests were analyzed with a Bonferroni correction to the alpha level. Except where mentioned, all analyses were done using the software JMP® 8.0 (SAS Institute Inc., Cary, NC).

3. Results and discussion

3.1. Hydraulic conductivity

All bioreactor treatments including the control increased in K_{sat} over time (Table 2). While it is possible that over long durations, K_{sat} would decrease as a result of wood degradation-induced compaction and biomass growth, in this study the fact that the sand-only treatment (control) also increased indicated that changes in hydraulic conductivity over the short-term may be driven by the formation of preferential flow channels. Robertson et al. (2009) found no evidence of K_{sat} decline in a sawdust-only bioreactor over 7 years. In a mesocosm experiment modeling denitrification beds (wood-only), Cameron and Schipper (2010) found that the hydraulic conductivity increased over the short-term in

Table 2
A statistical analysis of the mean and rate of change inhydraulic conductivity from varying the wood volume and particle size. Means ± 1 S.D. for the 246 days duration of the study are presented. ANOVA results indicate a significant difference within the treatment. Treatments with different letters are significantly different from each other at $p < 0.05$.

Wood volume treatment				Wood size treatment			
Vol (%)	Mean	ANOVA		Wood size	Mean	ANOVA	
Saturated hydraulic conductivity (K_{sat}) by treatment (cm min^{-1})							
0	1.9 ± 0.7		A	Shred	2.06 ± 0.6		A
10	1.55 ± 0.5	$F(3,17) = 0.6$, $p < 0.651$	A	Coarse	0.62 ± 0.3	$F(3,8) = 4.3$, $p < 0.043$	B
25	1.38 ± 1.0		A	Fine	2.14 ± 0.7		A
50	1.86 ± 0.8		A	Control	1.91 ± 0.7		A
Rate of change of saturated hydraulic conductivity by treatment (ΔK_{sat} yr^{-1})							
0	2.5 ± 0.2		A	Shred	2.04 ± 1.1		AB
10	1.7 ± 1.2	$F(3,20) = 0.3$, $p < 0.799$	A	Coarse	0.55 ± 0.5	$F(3,8) = 5.0$, $p < 0.029$	B
25	2.3 ± 2.1		A	Fine	4.36 ± 2.1		A
50	2.6 ± 1.8		A	Control	2.52 ± 0.2		AB

fine wood media in the range of the particles used in the present study, although they noted a marked decline in K_{sat} in coarser wood media that was attributed to the influence of differences in particle geometry and sorting on the trapping of gas bubbles.

Increasing the volume of all wood types (0%, 10%, 25% and 50% by volume) had no consistent effect on the mean hydraulic conductivity (Table 2). The hydraulic conductivity increased at a greater rate with higher wood volumes although the differences were not significant. Similarly there was no consistent trend in the mean or rate of change within the particle size treatment. The intermediate-size coarse sawdust had a lower mean and rate of change in hydraulic conductivity than the finer sawdust and the larger shredded pine. This study indicates the difficulty in predicting the influence of different mixtures of sand and wood particles with diverse geometry and sorting behavior on hydraulic connectivity trends that are influenced by complex factors including pore size distribution, and gas bubble transport.

3.2. Dissolved organic C and TKN export

The DOC export rate was calculated for each of the eight sampling events as the mass flux of DOC per volume of reactor media [M L^{-3} T^{-1}] and modeled over time to calculate a normalized total mass flux. The DOC export rate was initially high for all treatments and rapidly declined to a much lower asymptotic rate after approximately 50–150 days following an exponential decay curve (Fig. 2). Generally the total DOC export rate increased with increasing wood volume ratio, although the oak sawdust treatments were an exception (Table 3). The oak volume ratio increased from 0.25 to 0.50, although the DOC export rate was slightly lower in the latter treatment. This discrepancy could be explained by differences in hydraulic properties between the two oak treatments. Similarly to any mass flux, the DOC export rate is the product of the concentration of the analyte and the hydraulic loading rate and the correlation between K_{sat} and DOC export rate was significant in this study ($r^2 = 0.56$, $p < 0.03$) The K_{sat} of the 0.50 oak volume ratio treatment was lower than the 0.25 wood volume ratio treatment by 33% on average, which explained the incongruity. It should be noted that the long-term or asymptotic mass flux rate of the 0.50 oak volume ratio treatment was over 1.5 times greater than the 0.25 oak volume ratio treatment, which indicated that more leachable C remained at the end of the study (Table 3). Similarly, the coarse pine sawdust had lower DOC exports rates over time than the other treatments that likely resulted from a lower K_{sat} (Table 2). This indicates that denitrification bioreactors with high hydraulic loading rates will have higher DOC export rates.

There were no significant differences in TKN export between treatments ($F(8,567) = 1.2$, $p < 0.28$). Similarly to DOC concentration and mass flux, the TKN concentration declined exponentially over time (Fig. 3). A strong correlation between TKN and DOC concentration in effluent waters ($r^2 = 0.80$) indicates that a majority of the TKN was present as organic-N associated with leaching DOC. This correlation between DOC and TKN concentration declined over time and was not significant in the final two sampling events, which possibly indicated a change in source from physical leaching to biologically-driven processes.

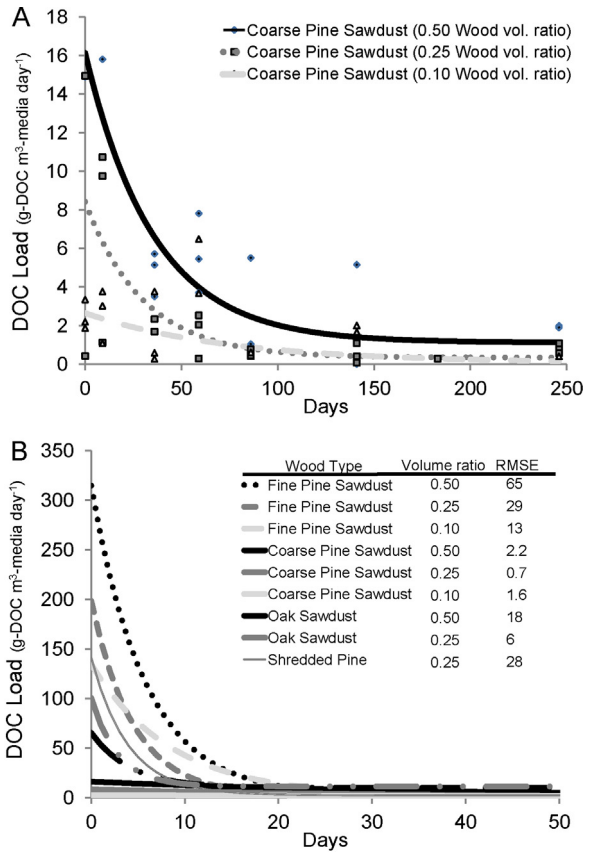

Fig. 2. Graphs of the change in dissolved organic C (DOC) flux rate per volume of bioreactor media over time for all treatments. Shown in the figure are (A) actual and modeled data of the coarse pine sawdust treatment as an example and (B) modeled data and root mean squared error (RMSE) for all the treatments. Regression coefficients for the modeled data are shown in Table 2 following Eq. (2).

Table 3
Actual and modeled values of average dissolved organic C (DOC) flux. The max DOC concentration, modeled total and long-term asymptotic DOC fluxrates per volume of media are displayed. The equation parameters (C_o, r, θ) for the DOC loading rate over time (Eq. (2)) as well as the root mean squared error (RMSE) of the model fit are reported.

Wood type (wood vol. density)	Max DOC conc. ($mg\,L^{-1}$)	DOC flux rate ($g\,m^{-3}$-media d^{-1})	Asymptotic rate ($g\,m^{-3}$-media d^{-1})	C_o	r	θ	RMSE
Fine pine sawdust (0.10)	429	942	0.49	134	0.18	0.49	12.5
Fine pine sawdust (0.25)	600	1220	1.00	197	0.22	1.00	29.1
Fine pine sawdust (0.50)	755	2109	0.53	314	0.17	0.53	64.9
Coarse pine sawdust (0.10)	27	268	0.40	2.70	0.01	0.06	1.6
Coarse pine sawdust (0.25)	124	394	0.43	14.9	0.05	0.43	0.7
Coarse pine sawdust (0.50)	272	748	0.67	15.3	0.03	0.62	2.2
Oak sawdust (0.25)	442	914	0.95	147	0.24	0.95	5.6
Oak sawdust (0.50)	392	820	1.47	87.4	0.20	1.47	17.6
Shredded pine (0.25)	531	725	0.32	141	0.24	0.32	27.5

3.3. Media carbon quality transformation

Total C concentration and fiber composition were quantified on the bioreactor media at the beginning and end of the study to determine differences in media quality degradation rates as a result of DOC leaching and microbial decomposition. Throughout the duration of the study (246 days), total C and non-lignin fiber content significantly declined by $31 \pm 21\%$ and $12 \pm 29\%$, respectively (Fig. 4). The proportion of the total C loss attributed to dissolved organic C export (Table 3) only ranged from 2 to 30% (average = $13 \pm 12\%$) amongst the different treatments, which indicated that a majority of the C was lost as gaseous emissions (CO_2 or CH_4) from microbial decomposition. Statistically significant reductions in NDF ($-0.57 \pm 0.37\%$, $n = 27$, $p < 0.001$), hemicellulose ($-0.56 \pm 0.54\%$, $n = 27$, $p < 0.001$) and cellulose ($-0.58 \pm 1.59\%$, $n = 27$, $p < 0.035$) as a percentage of total media were observed, while the recalcitrant ash and lignin proportions significantly increased ($1.1 \pm 1.9\%$, $n = 27$, $p < 0.025$). There were no significant differences in the loss rate between the non-lignin fiber components (NDF, cellulose, and hemicellulose), which indicated a relatively even consumption and export rate of all non-lignin fractions over the duration of the study.

In addition to the proportion of lignin and ash in the media, the lignocellulose index (LCI) (lignin/lignin + cellulose) is an indicator of organic matter bioavailability particularly under anaerobic conditions (DeBusk and Reddy, 1998). Organic matter in wetland soils stabilizes at an LCI of 0.8, after which the organic matter is highly recalcitrant under continued anaerobic conditions (DeBusk and Reddy, 1998). Within the treatments, the LCI was initially 0.25 ± 0.10 and increased to 0.44 ± 0.13 in the 246 day duration of the study, indicating that the media is still bioavailable but becoming more recalcitrant. These LCI values are very similar to the differences observed in a longer term denitrification wall study between day 0 (0.24) and day 540 (0.4 ± 0.04) (Schmidt and Clark, 2012a). Longer term studies are necessary to determine the utility of utilizing fiber components and the LCI index as an indicator of denitrification wall lifespan.

There were no significant differences in total C consumption between treatments (Table 4). Generally, there were no significant differences in the percent consumption of individual fiber components between wood type and wood volume ratio treatments, with the exception of the oak sawdust (Table 4). The lignin proportion of the oak sawdust significantly decreased over time, while this fraction increased as a proportion of total media in all the other treatments ($F(2,12) = 9.8$; $p < 0.003$). While anaerobic lignin

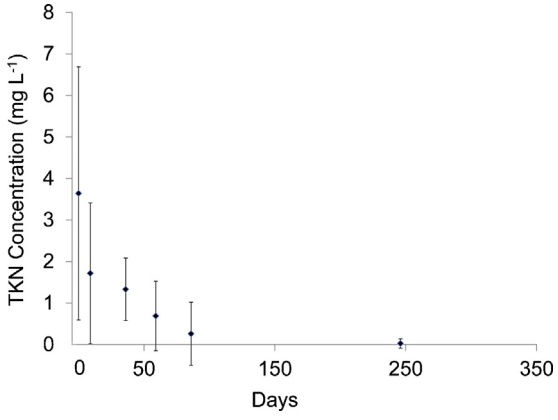

Fig. 3. The average of the TKN concentration ± 1 standard deviation in effluent water over the duration of the study.

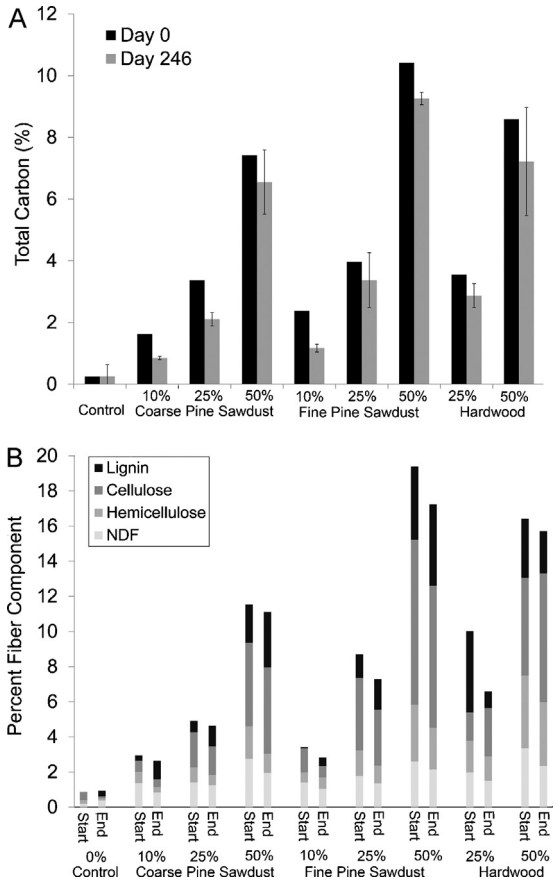

Fig. 4. Changes in C quantity and quality of the bioreactor media treatments over the duration of the study. Values shown are (A) percent total C and (B) percent total fiber proportions at the beginning and end of the study.

Table 4
A statistical comparison of the media carbon quality transformations between different treatments over the duration of the study. The change in % is the change relative to the total bioreactor mass (initial fiber or C mass-final fiber or C mass)/total bioreactor mass. ANOVA results indicate a significant treatment effect. Treatments with different letters in the Group column are significantly different from each other at $p < 0.05$.

Fiber type	Fiber change by wood volume ratio				Fiber change by wood type			
	Vol.	Change in %	ANOVA	Group	Type	Change in %	ANOVA	Group
NDF	0	+0.18 ± 0.1		B	Ctrl	+0.18 ± 0.2		B
	0.1	−0.43 ± 0.3	$F(3,17) = 5.0$	A	Soft	−0.43 ± 0.1	$F(2,12) = 11$	A
	0.25	−0.33 ± 0.3	$p < 0.011$	AB	Hard	−0.74 ± 0.4	$p < 0.002$	A
	0.5	−0.62 ± 0.4		A				
Hemicell.	0	−0.08 ± 0.2		B	Ctrl	−0.08 ± 0.1		B
	0.1	−0.10 ± 0.3	$F(3,17) = 4.5$	B	Soft	−0.46 ± 0.1	$F(2,10) = 4.6$	AB
	0.25	−0.32 ± 0.2	$p < 0.017$	AB	Hard	−0.56 ± 0.1	$p < 0.04$	A
	0.5	−0.78 ± 0.6		A				
Cellulose	0	−0.36 ± 0.1		A	Ctrl	−0.36 ± 0.1		AB
	0.1	−0.54 ± 0.3	$F(3,17) = 0.2$	A	Soft	−1.39 ± 1.1	$F(2,12) = 8.4$	A
	0.25	−0.81 ± 0.8	$p < 0.862$	A	Hard	+0.82 ± 1.0	$p < 0.005$	B
	0.5	−0.78 ± 1.4		A				
Lignin	0	+0.31 ± 0.5		A	Ctrl	+0.31 ± 0.5		B
	0.1	+0.58 ± 0.6	$F(3,17) = 0.9$	A	Soft	+0.66 ± 0.4	$F(2,12) = 9.8$	B
	0.25	+0.50 ± 0.2	$p < 0.448$	A	Hard	−2.0 ± 2	$p < 0.003$	A
	0.5	+0.69 ± 0.7		A				
%C	0	0			Ctrl	0		
	0.1	−0.99 ± 0.3	$F(2,15) = 0.5$	A	Soft	−0.62 ± 0.8	$F(1,10) = 0.5$	A
	0.25	−0.67 ± 0.9	$p < 0.601$	A	Hard	−1.02 ± 1.2	$p < 0.507$	A
	0.5	−1.0 ± 0.7		A				

decomposition in the oak media was not likely, the effluent from the oak treatments was much darker in color than the other treatments. Oak wood leachate has been found to have higher tannin, lignin, phenols and chemical oxygen demand than pine leachate (Svensson et al., 2013) and these properties have been found to increase the toxicity of wood leachate to aquatic organisms (Tao et al., 2005), which may be a concern when bioreactors are installed in close proximity to surface waters.

3.4. Denitrification reaction kinetics

If the denitrification rate was dependent on variations in nitrate concentration (first order reaction kinetics), then nitrate-reduction rates should have varied as groundwater flowed through the bioreactor and nitrate was depleted. Predictions and models of bioreactor performance will need to incorporate this non-linearity in denitrification rate. Contrastingly, if the nitrate reduction rate was independent of nitrate (zero order) then the reaction was dependent on other parameters such as enzyme kinetics, available C or inhibitory factors such as the presence of dissolved oxygen.

In this study, nitrate-N reduction rates appeared to be zero order with respect to nitrate-N. Even though nitrate-N concentrations declined as groundwater flowed through the mesocosms, there was no significant difference and no significant trend in nitrate-N reduction rates when compared between sampling ports within any groundwater temperature (Fig. 5a). Similarly, correlations between nitrate-N concentration and nitrate-N reduction rates were not significant and highly variable within each temperature. This is consistent with the experimental results of others who found zero order reaction kinetics with respect to nitrate-N (Robertson, 2010; Warneke et al., 2011b), although in a study of four field-scale denitrification beds, Christianson et al. (2012) found convincing evidence of first-order reaction kinetics. In this study, it is plausible that at very low nitrate-N concentrations, reaction rates declined as would be predicted by Michaelis–Mentin kinetics, but due to the distances between sampling locations this was undetected in the present study. Finer spatial-scale experiments are necessary to determine the kinetics of denitrification in bioreactors at low nitrate-N concentrations, although for practical application a linear zero order model appeared to be sufficient.

There was no observed lag in nitrate-reduction rates near the influent (0–38 cm) of the mesocosm, which indicated that C was sufficiently available and influent dissolved oxygen concentrations ($2.7 \pm 1.3\ mg\ L^{-1}$) were not present at inhibitory concentrations within the first 38 cm (~0.6 days). There were no consistent spatial variations in fiber consumption, although total C was significantly lower near the influent possibly indicating an increased consumption rate as a result of aerobic decomposition (data not shown). Although these experimental systems were not limited by nitrate, there was a variable but significant positive relationship between nitrate-N reduction rates and DOC flux (mass × discharge) ($r^2 = 0.30$, $p < 0.0001$) but not DOC concentration ($r^2 = 0.02$, $p < 0.10$), indicating that in flow-through systems, bacterial responses to nutrient limitation may be more strongly related to the rate of nutrient flux rather than concentration alone.

3.5. Denitrification rates of bioreactor media treatments

The average nitrate concentration in the influent was $7.5 \pm 0.73\ mg\ L^{-1}$ and the average effluent concentration from all treatments over all temperatures was $4.6 \pm 3.6\ mg\ L^{-1}$. Some of the nitrate-N entering the mesocosm could have been transformed to other N forms or stored within the media, although TKN mass flux and bioreactor media N increases were only a small fraction ($0.48 \pm 0.003\%$ and $2.1 \pm 6.0\%$ respectively) of influent nitrate concentration, which indicates that the majority of the influent nitrate-N was lost in gaseous form. This conclusion is strengthened when you consider that some of the TKN increases and media N enrichment may not result from transformations of influent nitrate, instead resulting from wood leaching and the preferential decomposition of carbon, respectively.

During the first three sampling periods (days 0, 9 and 36), the nitrate-N reduction rate was sufficient that no nitrate was present in even the first sampling port. Although this nitrate limitation precluded an exact determination of nitrate-N reduction rates, rates would necessarily be higher than $38\ g\ m^{-3}\ d^{-1}$ in one mesocosm

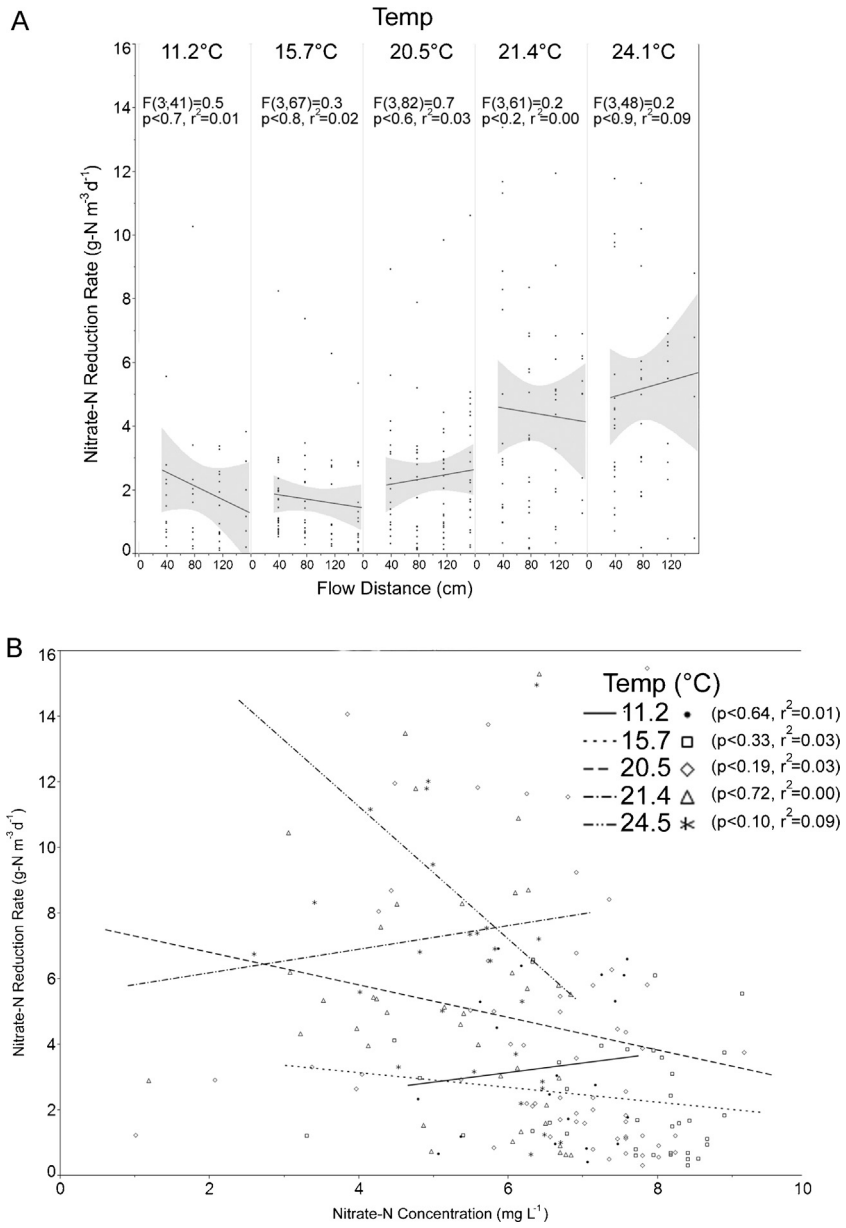

Fig. 5. Figures demonstrating the relationship between denitrification rate and nitrate-N concentration stratified by groundwater temperature. Shown in the figures are the (A) average NO_3-N reduction rate vs. distance from the inflow with best fit line and 95% confidence interval and (B) NO_3-N reduction rates as a function of NO_3-N concentration with best fit line. The significance values of the best fit lines are displayed.

and averaging greater than $9.3 \pm 6.2\,g\,m^{-3}\,d^{-1}$ over all the mesocosms. These exceptionally elevated nitrate-N removal rates were likely due to the high availability of labile dissolved organic C in fresh media at day 0, day 9 and day 36 (194 ± 173, 66 ± 70 and $28 \pm 26\,mg\,L^{-1}$, respectively) (Fig. 2) and high groundwater temperatures ($26.0 \pm 0.28\,^{\circ}C$). To minimize nitrate-N limitation and provide enduring measurements of nitrate-N reduction rates, the data from the first 60 days was excluded from this analysis and the flow-rate was increased for the duration of the study so that nitrate-N was still present in all the sampling ports. The average hydraulic residence time within the mesocosms for the duration of the study was 1.4 ± 3.0 days and the average pore water velocity was $291 \pm 274\,cm\,d^{-1}$.

Temperature influenced the denitrification rate of all the treatments. For the duration of the study, the average temperature of influent groundwater ranged from 7.9 to 24.1 °C and the absolute value of the average change in temperature between influent and effluent of the mesocosms averaged $3.3 \pm 2.1\,^{\circ}C$. The effect of temperature on the denitrification reaction for all treatments was quite strong ($r^2 = 0.87$) and described effectively by an exponential model (Fig. 6). The Q_{10} value across the temperature range of measurement (7.9–24.1 °C) was 4.7. The Q_{10} of many other denitrification bioreactor studies ranged from 0.16 to 3.5 (Cameron and Schipper, 2010; Elgood et al., 2010; van Driel et al., 2006a,b; Warneke et al., 2011b,c). Other studies examined over a comparatively wide range of temperatures as the present study have found Q_{10} values as high as 5.7 (Christianson et al., 2012) in denitrification beds, and Robertson et al. (2008) reported a Q_{10} value of 4.95 ($r^2 = 0.96$) in a denitrification wall over a similar temperature range as the present study (6–22 °C). Additionally the exponential rate constant (0.16) of the Robertson et al. (2008) study and the present work are equivalent. The Q_{10} value of biological reactions is

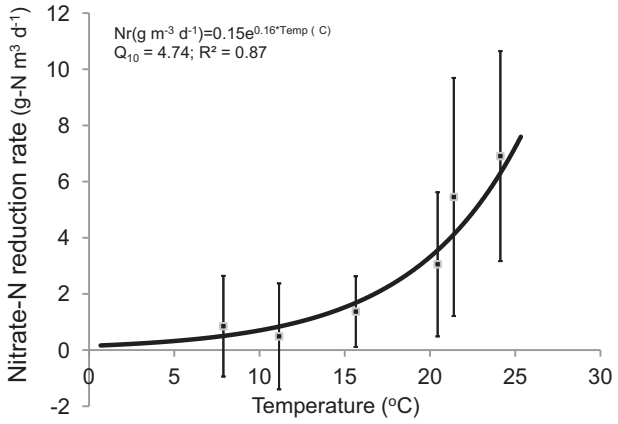

Fig. 6. The nitrate-N reduction rate as a function of groundwater temperature averaged for all the treatments.

commonly estimated with a value of 2.0, the higher Q_{10} values reported possibly indicated a synergistic response between increasing denitrification rates and other reactions that increased C availability with increasing temperatures.

The nitrate-N reduction rates of the different qualitative treatments were pooled and compared in three separate analyses to determine differences in denitrification rates among differing wood types, sizes and amounts alone. Because denitrification rates for a given treatment are not static and vary strongly with temperature, an analysis of covariance was used controlling for the covariate temperature. For all three comparisons (wood type, size and volume ratio), the treatment effect and temperature interaction were significant $F(3,156) = 6.8$, $p < 0.001$; $F(2,68) = 5.8$, $p < 0.005$ and $F(3,60) = 12$, $p < 0.0001$, respectively (Table 5). Although the overall temperature interaction was significant, some of the individual treatment-temperature interactions were variable as designated by p-values in Fig. 8. The whole model was relatively homoscedastic, significant for all three comparisons ($p < 0.0001$), and explained 52, 59 and 73% of the variability for the wood volume ratio, type and particle size treatments, respectively (Fig. 7). The relationship between temperature and nitrate-N removal rates within a given treatment for this statistical model could be calculated based on Eq. (3):

$$N_r = \alpha + bx + cx^2 \quad (3)$$

In this equation, N_r is the nitrate-N reduction rate per volume of reactor media [g-N m^{-3} of media d^{-1}], x is the temperature, α, b and c are the intercept, temperature regression coefficient and temperature quadratic term as shown in Table 5.

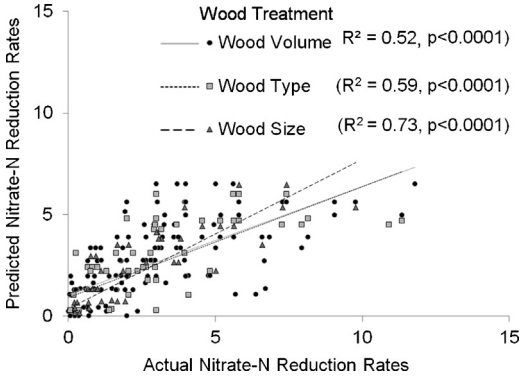

Fig. 7. Figure detailing the goodness of fit between the actual and predicted nitrate-N reduction rates of the ANCOVA statistical model for the wood volume ratio, type and particle size treatments.

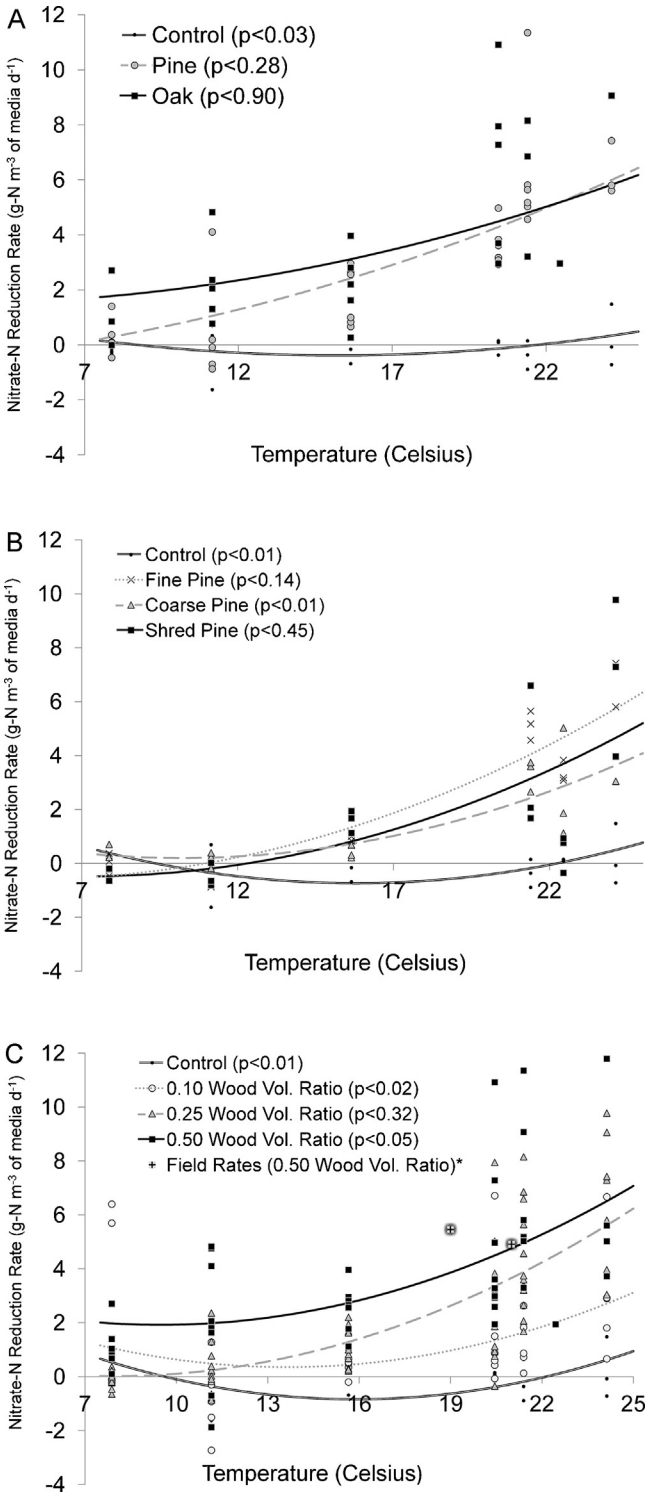

Fig. 8. The results of the ANCOVA model comparing nitrate-N reduction rates across a range of temperatures. Comparisons shown include the (A) wood type (B) size and (C) volume ratio treatments respectively. The rates measured in the field (Schmidt and Clark, 2012a) for the comparable treatment (0.50 Wood volume) are designated on the figure. p-Values for the temperature-treatment interaction are displayed.

The oak treatment had slightly higher nitrate-N reduction rates particularly at low temperatures, although the differences from pine sawdust were not significant overall (Table 5; Fig. 8a).

Table 5
A statistical analysis of the effects on nitrate-N reduction rate from varying the wood type, size and volume ratio. The wood treatments (type, size and volume ratio) were pooled to discern statistical differences. Least squares means ± 1 S.D. of nitrate-N reduction rate are presented as rate mass loss per volume of reactor media. The equation coefficients for the ANCOVA model (Eq. (3)) are also displayed. The coefficients α, b, and c listed underneath each pooled treatment were used to create the correlations with temperature in Fig. 8.

Wood volume ratio treatment				Wood type treatment				Wood size treatment			
Wood vol. ratio	NO_3-N removal rate ($g\,m^{-3}\,d^{-1}$)	ANOVA		Wood type	NO_3-N removal rate ($g\,m^{-3}\,d^{-1}$)	ANOVA		Pine size	NO_3-N removal rate ($g\,m^{-3}\,d^{-1}$)	ANOVA	
0	−0.14 ± 2.0		A	Control	−0.08 ± 1.9		A	Control	−0.07 ± 1.4		A
0.1	1.24 ± 2.1		AB	Soft	3.00 ± 2.0		B	Shred	1.86 ± 1.4		B
0.25	2.32 ± 2.0		BC	Hard	3.61 ± 2.1		B	Coarse	1.64 ± 1.5		B
0.5	3.68 ± 2.1		D					Fine	2.47 ± 1.5		B
Model	$r^2 = 0.52$	$F(8,157) = 21$ $p < 0.001$		Model	$r^2 = 0.56$	$F(6,69) = 15$ $p < 0.0001$		Model	$r^2 = 0.73$	$F(8,157) = 21$ $p < 0.0001$	
	α	*b*	*c*		α	*b*	*c*		α	*b*	*c*
0.10	4.33	−0.58	0.021	Soft	−0.76	0.06	0.009	Shred	0.42	−0.25	0.018
0.25	1.37	−0.34		Hard	1.53	−0.04		Coarse	2.05	−0.36	
0.5	3.84	−0.41						Fine	−0.09	−0.19	

ANOVA results indicate a significant difference within the treatment. Treatments with different letters in the group column are significantly different from each other at $p < 0.05$.

Similarly, although the fine pine sawdust had higher measured nitrate-N reduction rates than coarse pine sawdust and shredded pine across the majority of the temperature range, the differences between all the particle sizes were not significant (Table 5; Fig. 8b). This indicates that when considering the design of denitrification walls, variations in wood type (oak, pine) and wood grain size should not produce considerable differences in nitrate-N reduction rates, which confirms the results of others (Cameron and Schipper, 2010). Grouping all the various wood types in to the wood volume ratio treatment did produce significant differences in nitrate-N removal rates (Table 5; Fig. 8c). All the treatments were significantly different from the control with the exception of the 0.10 wood volume ratio and the nitrate-N reduction rates of the 0.25 and 0.50 wood volume ratio treatments were significantly different from each other and the 0.10 treatment (Table 5). The results from the denitrification wall (wood volume ratio = 0.50) receiving the same groundwater as the present study (Schmidt and Clark, 2012a,b) were within the realm of the model, although the model underpredicted actual field rates (Fig. 8c).

Because differences in wood type and size had no significant influence on nitrate-N reduction rates, the design of denitrification walls to achieve a desired nitrate reduction can be focused on the amount of wood alone. Relating the ANCOVA statistical models for nitrate-N reduction rates from variations in wood volume and groundwater temperature alone has great utility for providing design guidelines as shown in Fig. 9. If the influent N concentration and groundwater temperature are known, a detention time for complete nitrate removal can be quantified using these figures (Fig. 9). Based on the groundwater velocity and the desired detention time from Fig. 9, the appropriate denitrification wall flow-length can be determined.

3.6. Multivariate assessment of denitrification rate controls

Relationships between predictors measured at the beginning of the study and response variables were analyzed using bivariate correlations and multiple regression. Many of the metrics of C quality had significant bivariate correlations with average nitrate-N reduction rates and microbial biomass C (Table 6). The fiber analysis was an incremental procedure which extracted fiber components in order of liability from neutral detergent fiber (NDF), hemicellulose, cellulose and lignin. The two most labile fiber components NDF and hemicellulose were stronger predictors of nitrate-N reduction rates than measurements of C quantity alone (%C and %loss on ignition) (Fig. 10; Table 6). In contrast, microbial biomass C was less strongly correlated with labile fiber components and the microbial

Table 6
Correlations between initial measured predictors and nitrate-N reduction rate ($g\,m^{-3}\,d^{-1}$) and microbial biomass C ($mg\text{-}C\,kg^{-1}$)averaged over all temperatures. The Pearson correlation coefficients indicate the strength and the direction of the regression, while the *p*-value determines the significance of the relationship.

Nitrate-N reduction rate ($g\,m^3\,d^{-1}$)			Microbial biomass carbon ($mg\,kg^{-1}$)		
Denitrification rate predictor	Pearson correlation coefficient	*p*-Value	Microbial biomass predictor	Pearson correlation coefficient	*p*-Value
Neut. deterg. fiber (%)	0.75	<0.001	Cellulose (%)	0.74	<0.001
Surface area ($m^2\,g^{-1}$)	0.73	<0.001	Loss on ignition (%)	0.71	0.001
Hemicellulose (%)	0.70	<0.001	C (%)	0.70	0.001
Microbial biomass C	0.56	0.004	Hemicellulose (%)	0.59	0.003
C (%)	0.48	0.013	Neut. deterg. fiber (%)	0.56	0.004
Loss on ignition (%)	0.47	0.016	Surface area ($m^2\,g^{-1}$)	0.52	0.010
Cellulose (%)	0.45	0.021	Ave. NO_3 reduct. rate[a]	0.46	0.023
Potential DN rate[a]	0.35	0.089	Potential DN rate[a]	0.09	0.686
C:N ratio	−0.18	0.377	C:N ratio	−0.03	0.883

[a] Potential denitrification (DN) rate and the actual average NO_3 reduction rate have units of $g\text{-}N\,m^{-3}\,d^{-1}$.

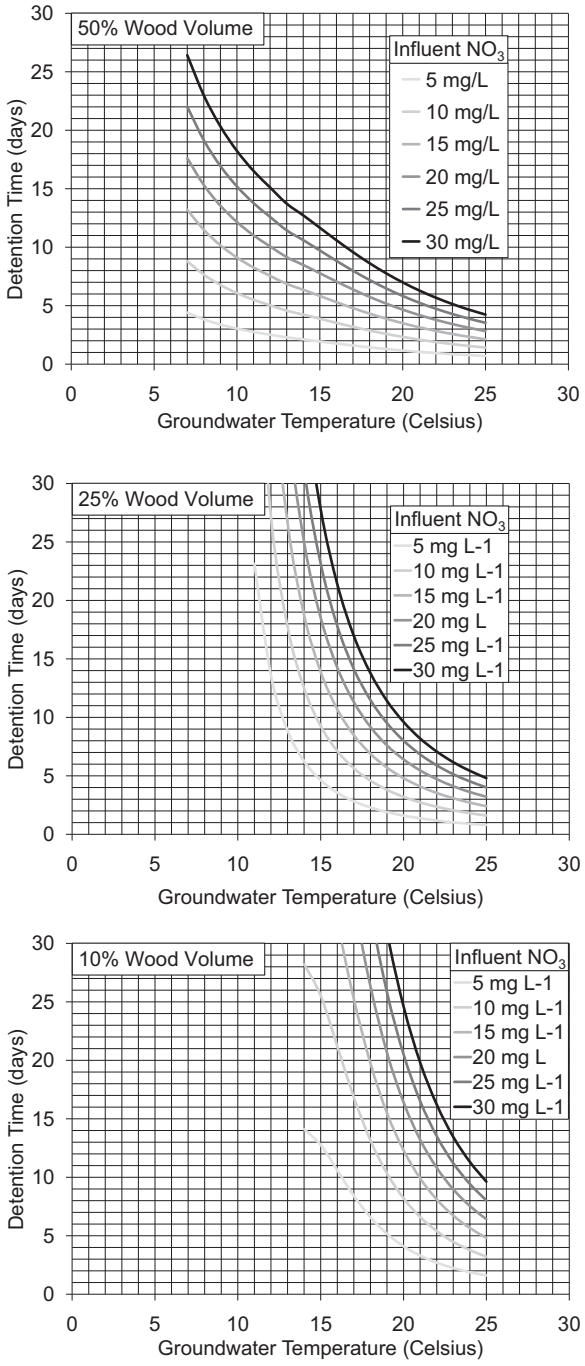

Fig. 9. Design guidelines relating the detention time required to completely remove influent NO_3 concentrations as a function of groundwater temperature for denitrification walls with wood to sand volumetric ratios of (A) 50%, (B) 25%, and (C) 10%. Based on the groundwater velocity and the desired detention time from this figure, the appropriate denitrification wall flow-length can be determined.

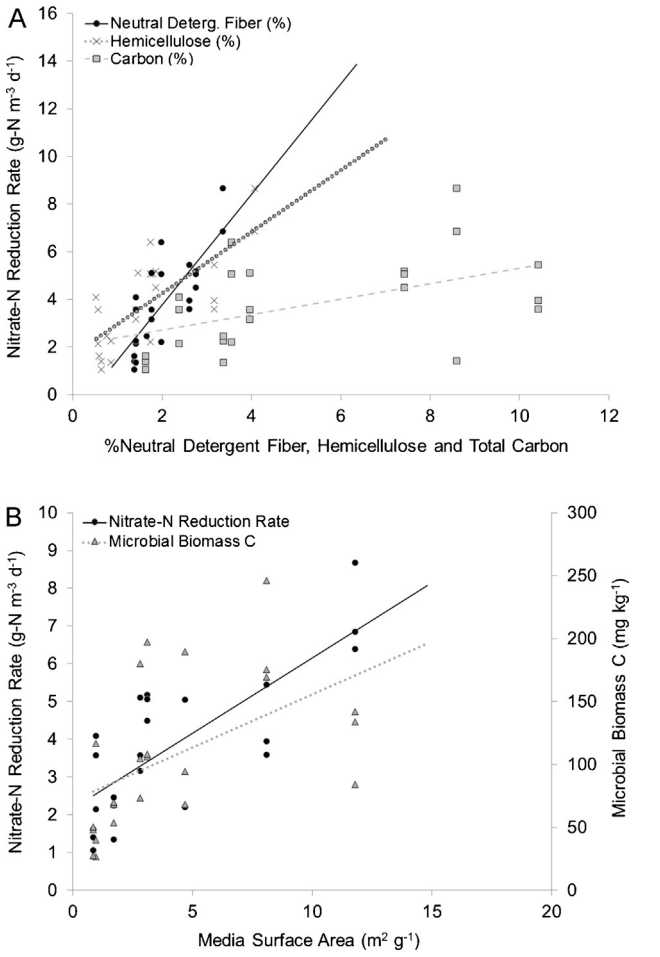

Fig. 10. Linear relationship between (A) nitrate-N reduction rate (g-N m^{-3} d^{-1}) and bioreactor media C quality (neutral detergent fiber, hemicellulose and total C) and (B) linear relationship between nitrate-N reduction rate (g-N m^{-3} d^{-1}) and media surface area (m^2 g^{-1}) and microbial biomass C (mg-C kg^{-1}).

population size was driven more strongly by total C quantity (Table 6). This indicates that there are differences in carbon and resource utilization between the bulk microbial population and the subset of this population which includes the denitrifiers. The C:N ratio, another metric of C quality was not strongly correlated with microbial biomass C or denitrification rate. In nitrogen rich aquatic systems, microbial populations may have less difficulty assimilating nitrogen and the C:N ratio may not be a strong indicator of microbial processes. Media micropore surface area was a very strong predictor ($r = 0.73$) of nitrate-N reduction rates, while less strongly predicting ($r = 0.52$) microbial biomass C (Fig. 10; Table 6). This discrepancy could result from the presence of chemolithoautorophic bacteria (methanogens, sulfur oxidizers, and anammox bacteria) which are not reliant on extracellular enzyme exposure to organic carbon as an electron donor or for cell biosynthesis like denitrifying bacteria. A large-scale colonization of a sulfur oxidizing bacteria of the *Beggiatoa* genus was previously described resulting from a denitrification wall installation and it is conceivable that methanogenic and anammox bacteria are present in these bioreactors. There was no significant relationship between potential denitrification rate and actual nitrate-N reduction rate. This indicates the utility of in situ studies as opposed to laboratory analyses for accurately quantifying relatively small differences in denitrification rate.

Using multiple regression, results were analyzed as a linear combination of predictor variables. Predictor variables were initially screened using a bidirectional stepwise multiple linear regression, which yielded neutral detergent fiber, micropore surface area, temperature and cellulose as predictor variables of significance. Temperature and surface area relationships were modified as non-linear exponential and logarithmic relationships, respectively. The final equation of this multiple regression model takes the form of Eq. (4):

$$N_r = b_1X_1 + b_2X_2 + b_3 \ln X_3 + b_4\, e^{eX_4} + a \quad (4)$$

Table 7
Parameters of the multiple regression model predicting nitrate-N removal rates as a function of temperature and media physicochemical properties. Nonstandardized coefficients (*b* coefficient), the standardized coefficient (beta wt.) and uniqueness index of the predictor variables are reported. The exponential constant (*r*) and intercept term (*a*) of the nonstandardized Eq. (4) are also shown.

Predictor	*b* coeffic.	SE *b* coeffic.	Beta weight.	*t*	Uniqueness index	*r*	*a*
Temp	0.127	0.07	0.71	13**	0.50	0.167	−3.7
Surface area	1.14	0.32	0.35	3.4**	0.032		
NDF	1.28	0.52	0.25	2.5*	0.017		
Cellulose	−0.194	0.099	−0.17	−2.0*	0.011		

* $p<0.05$.
** $p<0.001$.

Table 8
A comparison of actual field rates from a denitrification wall (Schmidt and Clark, 2012a) and the multivariate model predicted rates of the same media.

Temperature	Model predicted nitrate-N reduction rate	Average field nitrate-N reduction rate[a]	Max field nitrate-N reduction rate[a]
19	3.45	3.35	5.46
21	4.6	2.95	4.91

[a] Values are from Schmidt and Clark (2012a).

In this equation, N_r is the nitrate-N reduction rate per volume of reactor media [g m^{-3} d^{-1}] described in Eq. (1), X_1–X_4 are the actual measurements of NDF [%], Cellulose [%], surface area [L^2 M], and temperature [°C], respectively, b_1–b_4 are the constant coefficients of the respective predictors and α is the constant intercept term as reported in Table 7.

The results of the whole model were significant $F(5,133) = 36.3$, $p < 0.0001$, and explained approximately 67% of the variability (Fig. 11). The prediction accuracy was more variable at high nitrate-N reduction rates, with a tendency for the model to underestimate high rates. Beta weights (standardized multiple regression coefficients) and uniqueness indices were evaluated to determine the proportionate significance of each predictor variable (Table 7). The beta weight is a standardized estimate between −1 and 1, which indicated the direction and magnitude of the predictor variables influence on nitrate-N reduction rates and the uniqueness index is the percentage of variance accounted for by that predictor alone. Each of the predictor variables displays significant beta weights and uniqueness indices. The beta weights indicated that temperature was the strongest predictor of denitrification rate, followed by surface area, NDF and cellulose. The beta weight for cellulose was negative. Cellulose acted as a suppressor variable, which minimized irrelevant variability of other predictor variables.

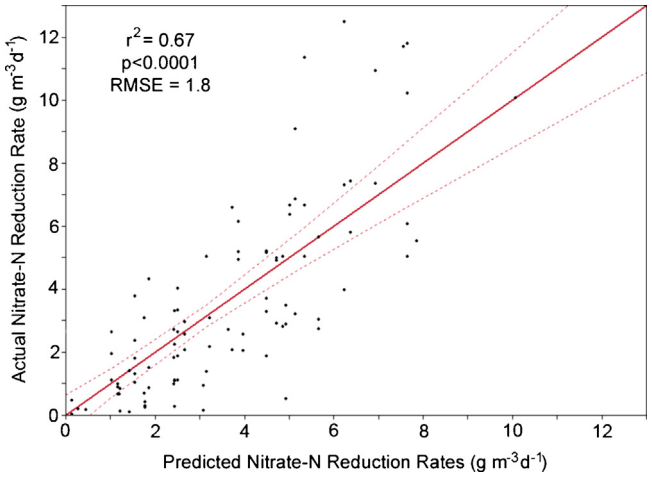

Fig. 11. Figure detailing the goodness of fit between the actual and predicted nitrate-N reduction rates of the multiple regression statistical model with a 95% confidence interval.

Temperature alone explained 50% of the variance in nitrate-N reduction rates, beyond the variance accounted for by the media properties (NDF, cellulose, surface area). This is similar to the multiple regression results from denitrification beds, where temperature was found to be the strongest driver of load reductions (Christianson et al., 2012). The other predictor variables accounted for 1–2% of the variability in this model each. It is possible that over time NDF will decline in importance for predicting N reduction rate as this bioavailable component is depleted. Although as discussed previously, over the short duration of this study all fiber components (NDF, hemicellulose, and cellulose) had equivalent rates of degradation and leaching. Additionally, bioreactor performance was only analyzed after the media had been leached for 60 days, which would exclude many temporarily labile C sources.

As described in the methods, two treatments were randomly chosen from each sampling day ($n = 12$), removed from model construction and compared as a linear regression to the model predicted values. Additionally the model was compared to rates measured in the field (Schmidt and Clark, 2012a) to verify the results. The relationship between model predicted and actual values for the verification dataset were strongly significant $F(1,10) = 145$, $p < 0.0001$, r^2 of 0.94. Although this is a limited dataset, the predicted rates from the model were relatively similar to average and maximum nitrate-N reduction rates measured in the field (Table 8). Further research is necessary to confirm the results of this model for accurately measuring field rates.

4. Conclusions

Modifications to wood particle size and type (oak, pine) did not markedly influence nitrate-N reduction rates, DOC leaching, or carbon degradation rates. Increasing the amount of wood used (wood volume ratio) and groundwater temperature significantly increased nitrate-N reduction rates and these factors alone can be used to design denitrification walls (Fig. 9). DOC mass flux rates generally increased with larger wood volume ratios and increased hydraulic loading rates. When a denitrification wall is to be located adjacent to sensitive surface waters, the wood volume ratio should be decreased and media hydraulic conductivity should be considered in addition to the desired nitrate removal (Fig. 9). The hydraulic properties of a given bioreactor media depend on the complex sorting of the range of wood particle sizes in to varying pore sizes, which precluded the development of normative conclusions in this study. Prior to denitrification wall construction it

will be important to quantify the hydraulic properties of each specific media using standard methods to minimize risk and assure the conductivity is higher than surrounding soils. Compounds in wood leachate have been found at levels which can be toxic to aquatic organisms. More research emphasis is necessary to assess the physicochemical properties and toxicity of different wood types and to determine the loss rates and sorption mechanisms of wood leachate DOC, in order to remediate these impacts and prescribe surface water buffer widths.

Utilizing a multivariate model, the relative influence of C quality, C quantity, temperature, and media surface area on denitrification rates was determined. Temperature alone was a dominant predictor variable that will most predominantly shape the dimensions of denitrification bioreactors and limit their geographical extent. Groundwater temperature is a relatively ungovernable property of a proposed bioreactor site. Within a given groundwater temperature range, the C quality and surface area of a chosen bioreactor media will influence denitrification rates. The C quality as measured by standard fiber composition analyses may be a useful metric for predicting denitrification rates, although longer-term research is necessary on the relationship between increases in soluble/bioavailable fiber components and denitrification wall longevity. Wood surface area was uniquely, positively correlated with nitrate-N removal rates, but increasing the wood size had no significant effect. This indicates that surface area measurements from gas sorptometry may be a more sensitive indicator of a biologically relevant surface area than grain size alone. The difficulty of measuring surface area and the limited relationship between surface area and particle size, will likely preclude the consideration of this variable in the design of denitrification walls.

Acknowledgements

We would like to thank the Florida Department of Environmental Protection (FDEP) and the Florida Department of Agriculture and Consumer Services for funding and Todd Stephens for allowing the research on his property. Additionally we would like to thank Patrick Moran and Cody Smith for field and lab assistance.

References

Ahuja, L.R., Naney, J.W., Green, R.E., Nielsen, D.R., 1984. Macroporosity to characterize spatial variability of hydraulic conductivity and effects of land management. Soil Science Society of America Journal l48 (July–August), 17 Ref.

ASTM Standard D2434, 2006, Standard Test for Permeability of Granular Soils (Constant Head). ASTM International, West Conshohocken, PA. DOI: 10.1520/D2434-68R06.

Barkle, G.F., Schipper, L.A., Burgess, C.P., Painter, B.D.M., 2007. In situ mixing of organic matter decreases hydraulic conductivity of denitrification walls in sand aquifers. Ground Water Monitoring and Remediation 28, 57–64.

Cameron, S.G., Schipper, L.A., 2010. Nitrate removal and hydraulic performance of organic carbon for use in denitrification beds. Ecol. Eng. 36, 1588–1595.

Christianson, L.A., Bhandari, A., Helmers, M., Kult, K., Sutphin, T., Wolf, R., 2012. Performance evaluation of four field-scale agricultural drainage denitrification bioreactors in Iowa. Trans. ASABE 55, 2163–2174.

DeBusk, W.F., Reddy, K.R., 1998. Turnover of detrital organic carbon in a nutrient-impacted Everglades marsh. Soil Sci. Soc. Am. J. 62, 1460–1468.

Elgood, Z., Robertson, W.D., Schiff, S.L., Elgood, R., 2010. Nitrate removal and greenhouse gas production in a stream-bed denitrifying bioreactor. Ecol. Eng. 36, 1575–1580.

Fahrner, S., 2002. Groundwater Nitrate Removal using a Bioremediation Trench. University of Western Australia, Perth (Honours Thesis).

Fetter, C.W., 2001. Applied Hydrogeology. Prentice-Hall, Upper Saddle River, NJ, USA.

Goolsby, D.A., Battaglin, W.A., 2000. Nitrogen in the Mississippi Basin; Estimating Sources and Predicting Flux to the Gulf of Mexico. U.S. Geological Survey, Reston, VA, USA.

Greenan, C.M., Moorman, T.B., Kaspar, T.C., Parkin, T.B., Jaynes, D.B., 2006. Comparing carbon substrates for denitrification of subsurface drainage water. J. Environ. Qual. 35, 824–829.

Hagy, J.D., Boynton, W.R., Keefe, C.W., Wood, K.V., 2004. Hypoxia in Chesapeake Bay, 1950–2001: long-term change in relation to nutrient loading and river flow. Estuaries 27, 634–658.

Howarth, R.W., Marino, R., 2006. Nitrogen as the limiting nutrient for eutrophication in coastal marine ecosystems: evolving views over three decades. Limnol. Oceanogr. 51, 364–376.

Jaynes, D.B., Kaspar, T.C., Moorman, T.B., Parkin, T.B., 2008. In situ bioreactors and deep drain-pipe installation to reduce nitrate losses in artificially drained fields. J. Environ. Qual. 37, 429–436.

Kilpelainen, A., Peltola, H., Ryyppo, A., Sauvala, K., Laitinen, K., Kellomaki, S., 2003. Wood properties of Scots pines (*Pinus sylvestris*) grown at elevated temperature and carbon dioxide concentration. Tree Physiol. 23, 889–897.

Long, L.M., Schipper, L.A., Bruesewitz, D.A., 2010. Long-term nitrate removal in a denitrification wall. Agric. Ecosyst. Environ. 140, 514–520.

Moorman, T.B., Parkin, T.B., Kaspar, T.C., Jaynes, D.B., 2010. Denitrification activity, wood loss, and N_2O emissions over 9 years from a wood chip bioreactor. Ecol. Eng. 36, 1567–1574.

Mukherjee, A., Zimmerman, A.R., Harris, W., 2011. Surface chemistry variations among a series of laboratory-produced biochars. Geoderma 163, 247–255.

Robertson, W.D., 2010. Nitrate removal rates in woodchip media of varying age. Ecol. Eng. 36, 1581–1587.

Robertson, W.D., Blowes, D.W., Ptacek, C.J., Cherry, J.A., 2000. Long-term performance of in situ reactive barriers for nitrate remediation. Ground Water 38, 689–695.

Robertson, W.D., Cherry, J.A., 1995. In situ denitrification of septic-system nitrate using reactive porous media barriers; field trials. Ground Water 33, 99–111.

Robertson, W.D., Vogan, J.L., Lombardo, P.S., 2008. Nitrate removal rates in a 15-year-old permeable reactive barrier treating septic system nitrate. Ground Water Monit. Remediation 28, 65–72.

Robertson, W.D., Ptacek, C.J., Brown, S.J., 2009. Rates of nitrate and perchlorate removal in a 5-year-old wood particle reactor treating agricultural drainage. Ground Water Monit. Remediation 29, 87–94.

Schipper, L., Vojvodic-Vukovic, M., 1998. Nitrate removal from groundwater using a denitrification wall amended with sawdust; field trial. J. Environ. Qual. 27, 664–668.

Schipper, L.A., Barkle, G.F., Hadfield, J.C., Vojvodic-Vukovic, M., Burgess, C.P., 2004. Hydraulic constraints on the performance of a groundwater denitrification wall for nitrate removal from shallow groundwater. J. Contam. Hydrol. 69, 263–279.

Schipper, L.A., Robertson, W.D., Gold, A.J., Jaynes, D.B., Cameron, S.C., 2010. Denitrifying bioreactors—an approach for reducing nitrate loads to receiving waters. Ecol. Eng. 36, 1532–1543.

Schipper, L.A., Vojvodic-Vukovic, M., 2001. Five years of nitrate removal, denitrification and carbon dynamics in a denitrification wall. Water Res. 35, 3473–3477.

Schmidt, C.A., Clark, M.W., 2012a. Efficacy of a denitrification wall to treat continuously high nitrate loads. Ecol. Eng. 42, 203–211.

Schmidt, C.A., Clark, M.W., 2012b. Evaluation of a denitrification wall to reduce surface water nitrogen loads. J. Environ. Qual. 41, 724–731.

Sparling, G.P., Feltham, C.W., Reynolds, J., West, A.W., Singleton, P., 1990. Estimation of soil microbial C by a fumigation-extraction method: use on soils of high organic matter content, and a reassessment of the k sub(EC)-factor. Soil Biol. Biochem. 22, 301–307.

Svensson, H., Marques, M., Kaczala, F., Hogland, W., 2013. Leaching patterns from wood of different tree species and environmental implications related to wood storage areas. Water Environ. J. 6, 214–220.

Tao, W., Hall, K.J., Masbough, A., Frankowski, K., Duff, S.J., 2005. Characterization of leachate from a woodwaste pile. Water Qual. Res. J. Can. 40, 476–483.

Tenkorang, F., Lowenberg-DeBoer, J., 2009. Forecasting long-term global fertilizer demand. Nutr. Cycl. Agroecosyst. 83, 233–247.

Tiedje, J.M., 1982. Denitrification. In: Page, A.L., et al. (Eds.), Methods of Soil Analysis. Part 2. Agron. Monogr, 2nd ed. ASA and SSSA, Madison, WI, pp. 1011–1026.

Timlin, D.J., Ahuja, L.R., Pachepsky, Y., Williams, R.D., Gimenez, D., Rawls, W., 1999. Use of Brooks–Corey parameters to improve estimates of saturated conductivity from effective porosity. Soil Sci. Soc. Am. J. 63, 1086–1092.

van Driel, P.W., Robertson, W.D., Merkley, L.C., 2006a. Denitrification of agricultural drainage using wood-based reactors. Trans. ASABE 49, 565–573.

van Driel, P.W., Robertson, W.D., Merkley, L.C., 2006b. Upflow reactors for riparian zone denitrification. J. Environ. Qual. 35, 412–420.

Van Soest, P.J., Robertson, J.B., Lewis, B.A., 1991. Methods for dietary fiber, neutral detergent fiber, and nonstarch polysaccharides in relation to animal nutrition. Journal of dairy science 74, 3583–3597.

Vance, E.D., Brookes, P.C., Jenkinson, D.S., 1987. An extraction method for measuring soil microbial biomass C. Soil Biol. Biochem. 19, 703–707.

Warneke, S., Schipper, L.A., Bruesewitz, D.A., Baisden, W., 2011a. A comparison of different approaches for measuring denitrification rates in a nitrate removing bioreactor. Water Res. 45, 4141–4151.

Warneke, S., Schipper, L.A., Bruesewitz, D.A., McDonald, I., Cameron, S., 2011b. Rates, controls and potential adverse effects of nitrate removal in a denitrification bed. Ecol. Eng. 37, 511–522.

Warneke, S., Schipper, L.A., Matiasek, M.G., Scow, K.M., Cameron, S., Bruesewitz, D.A., McDonald, I.R., 2011c. Nitrate removal, communities of denitrifiers and adverse effects in different carbon substrates for use in denitrification beds. Water Res. 45, 5463–5475.